An Improved Control Strategy to Microgrid Load Demand Sharing

S. Muqthiar Ali, Assistant Professor, Dept. of EEE A.I.T.S–RAJAMPETA,A.P,INDIA.
B. Madhan Mohan, Assistant Professor , Dept. of EEE A.I.T.S–RAJAMPETA,A.P,INDIA.
K. Ashok PG student(EPE), Dept. of EEE A.I.T.S-RAJAMPETA,A.P,INDIA

Abstract: **For the successful operation of self-governing microgrids the load demand sharing between the distributed generation (DG) units is an important task. In the parallel operation of DG units the frequency- voltage droop control and its various control methods have been reported in the literature, to achieve satisfied power sharing without communication between the DG units. However, due to mismatched feeder impedance the conventional droop control is subject to steady-state real and reactive power coupling steady-state reactive power sharing errors in the low voltage microgrid. Hence, for the composite (meshed or looped) microgrid the reactive power sharing is more challenging to do. In order to improve the reactive power sharing accuracy, this paper proposes an improved control strategy that will guesses the reactive power control error by injecting small real power disturbances, which will be activated by giving the low-bandwidth synchronization signals from the central controller. A slow integration term simultaneously is also be added to the conventional droop control for elimination of reactive power sharing error. The proposed compensation method will accomplishes precise reactive power sharing at the steady state as same as the performance of real power sharing through frequency droop control. Simulation results obtained using MATLAB software will validate the feasibility of the proposed method.**

Keywords **- Distributed generation (DG), droop control, low bandwidth communication, microgrid, improved compensation method, real and reactive power sharing.**

I INTRODUCTION

The Distributed generation, also called on-site generation, dispersed generation, decentralized generation, distributed energy or district energy, generates electricity from many small energy sources. DG by delivering clean and renewable energy close to customers last can ease the strains of many conventional transmissions and distribution infrastructures [1].

However due to insight of power electronics based DG units also introduces a few issues, such as system resonance, protection disturbance, etc. these problems will degrade the reliability of power supply. Hence in order to overwhelm these, the microgrid concept has been proposed which is accomplished through the control operation of multiple DG units. In comparison with a single DG unit the microgrid can accomplish the better power management system within its distribution network by overcoming reliability and economical issues. Thus the better opportunity of microgrid is considered to pave to the future smart grid [1].

In an autonomous microgrid the total demand must be in the right manner shared by multiple DG units. The parallel operation of DG units is mainly based on the droop method. Conventionally, the frequency-and voltage magnitude control is adopted which mainly aims to accomplish the microgrid power sharing in a decentralized manner [6], [11], [15]-[18] ,[20],[21]. The DG feeders are mainly resistive hence, due to non-trivial feeder impedance the droop control governed microgrid is having tendency to some power control stability problems [2]. It can be observed that the real power sharing is while the reactive power sharing at steady state is sensitive to affects of non-trivial feeder impedance [3],[5],[7]. Furthermore, the existence of local loads and in the complex microgrid configurations reactive power sharing problems will be increased and the problem is more severe.

The power control issues are have been solving by few improved methods. In [1] and [2], the virtual frequency–voltage frame and virtual real and reactive power concept were developed, which improve the stability of the microgrid system. But the methods cannot subdue the reactive power sharing simultaneously. Hence the reliability of power is poor. In addition, when small scale synchronous generations united into a whole microgrid right manner of power sharing between the DG units will become more challenging in these existing methods. In [3], both the reactive power and the harmonic power sharing errors were reduced with the non characteristic harmonic current injection. Despite the fact that the power sharing problem was addressed proportionate steady-state voltage distortions put down the microgrid power quality. In [4], a "*Q–V* dot droop" method was presented. It can be ascertained from this the betterment of reactive power sharing is not easily perceived or understood when local loads are considered to include. For forbidding the power control stability in [5]-[8] most frequent virtual output inductor is placed at the DG output terminal. In [7],[14], virtual impedance frame concept the reactive power sharing errors can be further reduced through an interesting model-based droop slope modification scheme. The method has capability to address the power control stability and power sharing errors simultaneously. It is the bright way to provide of high microgrid performance. Nevertheless, it is worth mentioning that the aforesaid virtual impedance control methods were developed based on uncomplicated microgrid configurations. So, due to the "plug-and-play" feature of DG units and loads [7], the microgrid configuration also changes with time. Without the real-time info of the microgrid configuration, virtual impedance control may not work properly as desired.

In response to the grid connected to the autonomous microgrid the right manner of control challenges, this paper presents an elementary reactive power sharing compensation scheme. The proposed method first up all identifies the

reactive power sharing errors through injecting small real-reactive power coupling disturbances, which are activated by the low-bandwidth synchronization flag signals from the central controller. Then the precise reactive power sharing is achieved by influencing the injected transient real-reactive power coupling using an intermittent integral control. With this proposed method reactive power sharing errors are significantly reduced. Once, the compensation over the proposed droop controller will be in a reflex manner switched back to the conventional droop controller. Note that the proposed accurate power control method is effective for microgrids with all types of configurations and load locations, and elaborated microgrid info is not needed in the proposed method to obtain the price power control. Simulation results are provided to verify the proposed load demand sharing method.

II ANALYSIS OF THE CONVETIONAL DROOP CONTROL METHOD

2.1 Operation of Microgrid

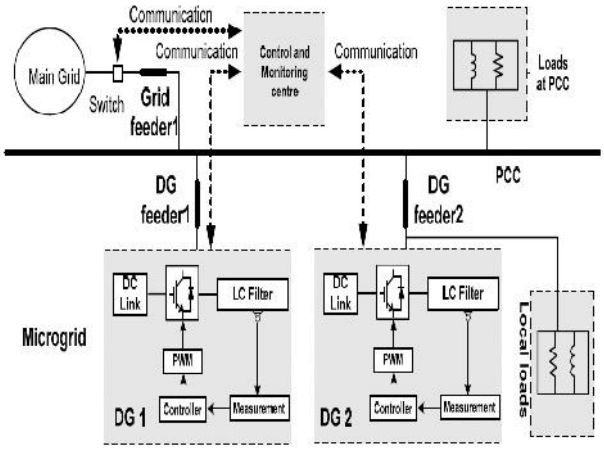

Fig. 1: Illustration of simple microgrid

The Fig. 1 illustrates strucrure of a simple microgrid. As shown, the microgrid is composed of as many as we required number of DG units and loads. Each DG unit is interfaced to the microgrid with an inverter, and the inverters are connected to the common ac bus through their respective feeders. This paper mainly focuses on the real and reactive power control by considering that the loads considered in the grid are nonlinear loads. The secondary controller [14], continuously monitors the relative status of the microgrid and main grid. As of requirement the microgrid can be connected to main grid (grid- connected mode) or disconnected (islanding mode) from the main grid through the control of static transfer switches (STS) at point of common coupling (PCC). In the grid-connected mode of operation, real and reactive power references are usually assigned by the central controller and the conventional droop control method can be used for power tracking. By contrast, to eliminate the steady-state reactive power tracking errors, the proportional plus integral (PI) regulation for the voltage magnitude control was developed in [7] and [11]. Thus, power sharing is not a real concern during the grid-connected operation. When the microgrid is switched to islanding operation, the entire load demand of the microgrid must be in the right manner shared by these DG units.

During the islanding operation, DG units as illustrated in Fig.1 can operate using the conventional real power–frequency droop control and reactive power–voltage magnitude droop control as

$$\omega = \omega_0 - D_P * P \qquad (1)$$

$$E = E_0 - D_Q * Q \qquad (2)$$

Where ω_0 and E_0 are the nominal values of DG angular frequency and DG voltage magnitude, *P* and *Q* are the measured real and reactive powers after the first-order low-pass filtering (LPF), *DP* and *DQ* are the real and reactive poweri droop slopes. With the derived angular frequency and voltage magnitude in (1) and (2), the instantaneous voltage reference can be obtained accordingly.

2.2 Reactive power sharing analysis

It is very difficult to share the reactive power in complex microgrid. For the reason of simplicity, this section first considers a uncomplicated microgrid with two DG units at the same power rating. The configuration is shown in Fig. 2(a), where each DG unit has a local load. R_1 and X_1 , and R_2 and X_2 are the feeder impedances of DG1 and DG2, respectively. In addition considering that DG units are often equipped with series virtual inductors to ensure the stability of the system, the corresponding equivalent circuit is outlined in Fig. 2(b).

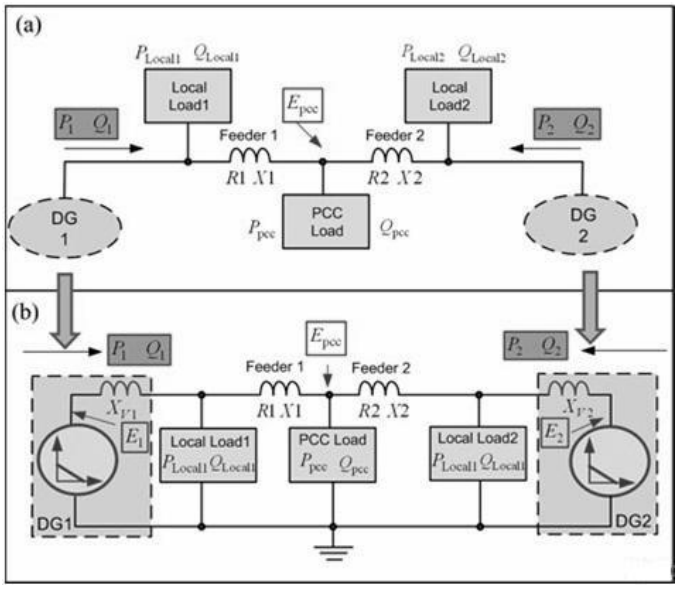

Fig. 2: Power flow in a simple microgrid: (a) configuration of the microgrid; (b) equivalent circuit model considering a virtual impedance control.

As shown, the virtual reactances X_{V1} and X_{V2} are placed at the outputs of voltage sources. The magnitudes of the voltage sources are obtained in (3) and (4) as

$$E_1 = E_0 - D_Q * Q_1 \qquad (3)$$

$$E_2 = E_0 - D_Q * Q_2 \qquad (4)$$

where E_1 and E_2 are the DG voltage magnitudes regulated by the droop control, and $Q1$ and $Q2$ are the output reactive powers of DG1 and DG2, respectively.

For the power flowing through either physical or virtual impedance, its accompanying voltage drop on the impedance yields the following approximation as

$$\Delta V \approx \frac{(X*Q)+(R*P)}{E_0} \qquad (5)$$

where P and Q are the real and reactive powers at the power sending end of the impedance, R and X are the corresponding resistive and inductive components of the impedance, E_0 is the nominal voltage magnitude, and ΔV is the voltage magnitude drop on the impedance.

Applying the voltage drop approximation in (5) to the present system in Fig. 2(b), the relationships between DG voltages (E_1 and E_2) and the PCC voltage (E_{PCC}) are established in (6) and (7) as

$$E1 = E_{pcc} \frac{X_1 \left(Q_1 - Q_{Local\,1}\right) + R_1(P_1 - P_{Local\,1})}{E_0} \qquad (6)$$

$$E2 = E_{pcc} \frac{X_2 \left(Q_2 - Q_{Local\,2}\right) + R_2(P_2 - P_{Local\,2})}{E_0} \qquad (7)$$

Important to remember that with system frequency as the communication link, the real power sharing using the conventional droop control is always precise [7]. Therefore, for the illustrated system at the steady state, the output real powers of DG1 and DG2 are obtained as

P1 = P2 = 0.5 , PTotal = 0.5 (Ppcc + PLocal1 + PLocal2 +PFeeder1+PFeeder2)

where *P*Total means the real power demand within the islanded microgrid, and *P*Feeder1 and *P*Feeder2 are the real power loss on the feeders. Similarly, the reactive power demand (*Q*Total) is defined as

QTotal = Qpcc + Q Local1 + QLocal2+QFeeder1+QFeeder2

where *Q*Feeder1 and *Q*Feeder2 are the reactive power loss on the feeders.

By solving the having formulas from (3) to (7), the reactive power sharing error (*Q*1−*Q*2) can be determined by mathematical computation.

It can be observed that the reactive power sharing error is related to a few factors, which include the commencement of local loads, unequal voltage drops on virtual and physical impedances, and the droop slope *DQ* variation. When all these factors are considered simultaneously, the evaluation of DG reactive sharing errors is not very easy even only two identical

DG units are included in the analysis. Due to the complexness of the circuit model, the forceful consequences of different factors shall be studied separately. For example, the impacts of unequal feeder reactance to reactive power sharing error can be studied by ignoring the effects of local loads, feeder resistance, and virtual impedance.

Fig.3, exhibits the reactive power sharing performance with mismatched feeder reactance, where the ideal inductive feeder leads to a linear relationship between the DG output

reactive power and the magnitude difference between PCC voltage (Epcc) and DG voltages (E_1 and E_2).

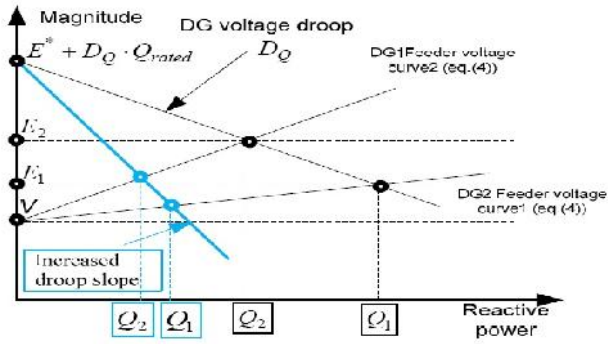

Fig. 3: Reactive power sharing of two DG units with mismatched feeder reactance.

The relationships are named as "DG1 feeder characteristics" and "DG2 feeder characteristics" in the figure. As shown, with mismatched feeder reactance ($X_1 < X_2$), the output reactive power of DG unit1 (Q_1) is higher than that of DG unit2 (Q_2) even the same droop slop (D_Q) is adopted for both DG units. It is observed that deeper droop slope D^*_Q might alleviate the reactive power sharing errors. However, as DG unit2 has larger feeder impedance, DG unit2's reactive power Q2 is smaller than Q1. An increased droop slope alleviates this problem, where the difference between Q1 and Q2 is reduced. However, steep slopes may lead to poor stability performance, which makes the microgrid system less reliable.

III PROPOSED REACTIVE POWER SHARING ERROR COMPENSATION METHOD

As we seen the reactive power sharing errors are caused by a number of factors and microgrids often have complex meshed configurations, developing the circuit model-based reactive power sharing error compensation scheme is not easy. Hence the main objective of this paper is to develop an enhanced compensation method that can get rid of the reactive power sharing errors without knowing the detailed microgrid structure. This feature is very important to accomplish the "plug-and-play" operation of DG units and loads in the microgrid.

3.1 Proposed compensation control:

The aim of this section is to develop a robust control method that can compensate the reactive power sharing error at steady-state. To initialize the compensation, the proposed compensation method adopts a low-bandwidth communication cable between the control and monitoring center and DG units. This communication channel will send out the compensation staring signals, so all DG units can start the compensation at the same time. Considering that the monitoring center also sends power reference signals in grid connected mode and the synchronization signals during operation mode transition. Note that only one way communication from the control and monitoring centre to the DG units is needed and the communication between DG units is not necessary for the implementation of this method. The proposed power control strategy is realized through the following two stages.

Stage 1: Initial power sharing using conventional droop method

Stage 2: Power sharing improvement through synchronized compensation

Stage 1: At first, by conventional droop method controller (1) and (2) are adopted for initial load power sharing before receiving compensation flag signal. In addition, the digital controller identifies the status of compensation starting flag dispatched from the microgrid monitoring center. Meanwhile, the DG local controller monitors the status of the compensation flag dispatched from the microgrid central controller. The steady staste averaged real power (P_{AVE}) in measured during this stage and it is used in stage 2. Due to consideration of system stability the cut-off frequency LPF's cannot be made very low to get the ripple free averaged real power (P_{AVE}). A moving average filter is used here to filter out the power ripples if any presented (see Fig4.). The measured average real power (P_{AVE}) is also saved in this stage, so that when the synchronization signal flag changes, the last saved value is used for a reactive power sharing accuracy improvement control in Stage 2.

Stage 2: Once a compensation starting signal is received by the DG unit, the average real power detection block stops updating, and the saved data P_{AVG} before receiving the compensation signal is obtained as a reference during

compensation. In the compensation process, a combination of

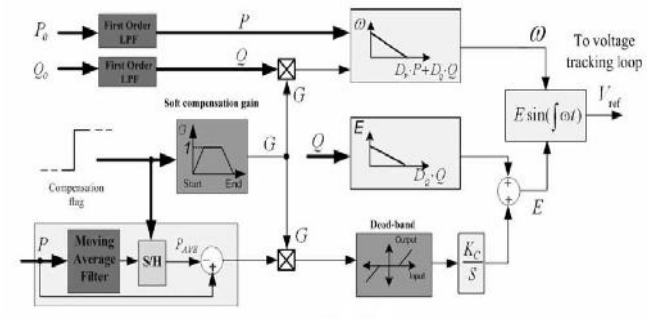

Fig.4: An enhanced reactive power compensation method

real and reactive power is used in frequency droop control (8), and the reactive power error is suppressed by using an additional integration term (9).

$$\omega = \omega_0 - (D_P*P + D_Q *Q) \quad (8)$$

$$E = E_0 - D_Q* Q + (K_C/S) * (P - P_{AVG}) \quad (9)$$

where K_C is the integral gain, which is selected to be the same for all the DG units.

It is observed that with the control strategy in Eqn. (8), the real and reactive power is coupled together for the frequency droop control. Compared to the conventional droop control, the reactive power droop term (D_Q*Q) in (8) is considered as an offset for the conventional real power droop control for frequency regulation. If there are any reactive power errors, the unequal offsets (D_Q *Q) from different DG units affect the DG output frequencies, which subsequently introduce the real power disturbances. This real power disturbance then cause the integral control term in (9) to regulate the DG output voltage. With this integral control, the real power from a DG eventually is equal to P_{AVE}, meaning that accurate real power sharing is still maintained in Stage. Further consider that the modified frequency droop control in (8) essentially enables equal sharing of the combined power (D_P *P + D_Q *Q) in Stage 2. The accurate sharing of both the combined power and real power means that the reactive power sharing will also be accurate.

For instance, with the proposed control in (8), the DG units providing less reactive power in Stage 1 experience a transient real power increase in Stage 2. Therefore, an integration of the real power difference ($P-P_{AVE}$) in a voltage magnitude control of (9) is able to eliminate the reactive power sharing error as discussed previously. Once the reactive power is shared properly, the DG unit real power flow go back to its original value with the control of (8), and the integration control used in (9) no longer contribute to the voltage magnitude regulation. To limit the impacts of small real power demand variations during the compensation transient, a dead band is placed before the integral control of the real power difference ($P-P_{AVE}$). To avoid the impacts of large load demand variations or load switching in a microgrid, the compensation period should be properly designed by tuning the integral gain (K_C) in (9). A long compensation period subject to possible microgrid load demand changes, while a too fast compensation lead to excess transient and affect the accuracy as well. Considering that the variation of microgrid load demand, such as that in the residential area microgrid, is normally slow [12]. Hence a compensation time of a few seconds in Stage 2 is considered. Finally, the soft compensation gain and the dead band block are installed at the DG unit local controller. Also the compensation time (2 s in the simulations) is preset in the DG unit local controller and it is the same for all the DG units in the microgrid. Therefore, only the synchronized compensation start signals are required for the proposed controller.

3.2 Small signal stability analysis:

Small-signal stability is defined as the ability of a power system to maintain its synchronism after being subjected to a small disturbance. The characteristics of a power system can be obtained by small signal analysis [22] using linear techniques.

3.2.1 for reactive power sharing error compensation method

The stability of DG units during the compensation process is investigated by small-signal stability analysis [10], [22]. First, the power flow of the DG unit is obtained as,

$$P = (EVY \cos\theta - V^2 Y) \cos\Phi - EVY \sin\Phi \sin\theta \quad (10)$$

$$Q = (V^2 Y - EVY \cos\theta) \sin\Phi - EVY \cos\Phi \cos\theta \quad (11)$$

where Y and Φ are the magnitude and angle of DG feeder admittance; E and V are the voltage magnitude at the DG unit output and the installation point, respectively. Θ is the power angle.

Accordingly, real and reactive power variations according to DG voltage disturbances are obtained in (12) and (13) as,

$$\Delta P_0 = K_{P\Theta}\,\Delta\Theta + K_{PE}\,\Delta E \quad (12)$$

$$\Delta Q_0 = K_{Q\Theta}\,\Delta\Theta + K_{QE}\,\Delta E \quad (13)$$

where P_0 and Q_0 are the instantaneous output powers of the DG unit, the operator Δ means small-signal disturbance around the DG system equilibrium point, $K_{P\Theta}$, K_{PE}, $K_{Q\Theta}$, and K_{QE} represent the power flow sensitivity to voltage angle and magnitude regulation.

When there are some power fluctuations during the compensation, by expanding the proposed compensation method in Eqns. (8) and (9), the small-signal response of the DG voltage is expressed from (14) to (17) as

$$\Delta P = \frac{\tau}{(s+\tau)}\Delta P_0 \quad (14)$$

$$\Delta Q = \frac{\tau}{(s+\tau)}\Delta Q_0 \quad (15)$$

$$\Delta\omega = -D_P\,\Delta P - D_Q\,\Delta Q \quad (16)$$

$$\Delta E = -D_Q\,\Delta Q + (K_s/s)\,\Delta P \quad (17)$$

where τ is the time constant of LPFs used in the power calculation.

Now from equations (14) to (17) express Δω and ΔE as,

$$\Delta\omega = -\frac{1}{s\tau+1}[(D_P K_{P\Theta} + D_Q K_{Q\Theta})\,\Delta\Theta + (D_P K_{PE} + D_Q K_{QE})\,\Delta E] \quad \ldots\ldots \quad (18)$$

$$\Delta E = \frac{K_C K_{P\Theta} - sD_Q K_{Q\Theta}}{s(s\tau+1) + sD_Q K_{QE} - K_C K_{PE}}\,\Delta\Theta \quad (19)$$

by substituting equation (19) in Eqn. (18) Δω is obtained as,

$$\Delta\omega = -\frac{1}{s\tau+1}\left[(D_P K_{P\Theta} + D_Q K_{Q\Theta})\,\Delta\Theta + \frac{(D_P K_{PE} + D_Q K_{QE})(K_C K_{P\Theta} - sD_Q K_{Q\Theta})}{s(s\tau+1) + sD_Q K_{QE} - K_C K_{PE}}\right]\Delta\Theta \quad (20)$$

The closed-loop characteristic equation is obtained by solving and replacing $\Delta\omega = s\,\Delta\Theta$,

$$s^4 + A\,s^3\,\Delta\Theta + B\,s^2\,\Delta\Theta + C\,s\,\Delta\Theta + D = 0 \quad (21)$$

where

$$A = \frac{\tau D_Q K_{QE} + 2\tau}{\tau^2} \quad (22)$$

$$B = \frac{-\tau K_C K_{PE} + D_Q K_{QE} + D_P K_{P\Theta}\tau + D_Q K_{Q\Theta}\tau + 1}{\tau^2} \quad (23)$$

$$C = \frac{D_Q K_{Q\Theta} - D_P K_{PE} D_Q K_{Q\Theta} - K_C K_{PE} + D_P K_{P\Theta} + D_P K_{P\Theta} D_Q K_{QE}}{\tau^2} \quad (24)$$

$$D = \frac{-D_Q K_{Q\Theta} K_C K_{PE} D_Q K_{Q\Theta} + D_Q K_{P\Theta} K_C K_{QE}}{\tau^2} \quad (25)$$

The homogeneous equation (21) describes the free motion of the system for small disturbances around equilibrium point. Then, the system response is analyzed by the characteristic equation (26).

$$\lambda^4 + A\,\lambda^3 + B\,\lambda^2 + C\,\lambda + D = 0 \quad (26)$$

The performances of the system with different control parameters are shown from Figs. 5–6. The DG unit circuit parameters are selected to be the same as in the simulation, and are listed in Table I. Fig. 5 shows the performance of the system using the conventional droop control method, where the real power droop gain *DP* is fixed while the reactive power droop slope *DQ* increases from 0.001 to 0.00433. As illustrated, it is a three-order system and the dynamic performance of the system is mainly determined by the dominate poles $\lambda 2$ and $\lambda 3$. It can be seen that the positions of the dominate poles are not sensitive to the variations of reactive power droop slope within the given range.

During the compensation process, the response of the system to different reactive power droop slopes (*DQ*) is also depicted

in Fig. 6. In contrast to the conclusions from Fig. 5, the DG unit becomes a fourth-order system in this case. Once again, the performance of system is evaluated by the dominate pole approximation.

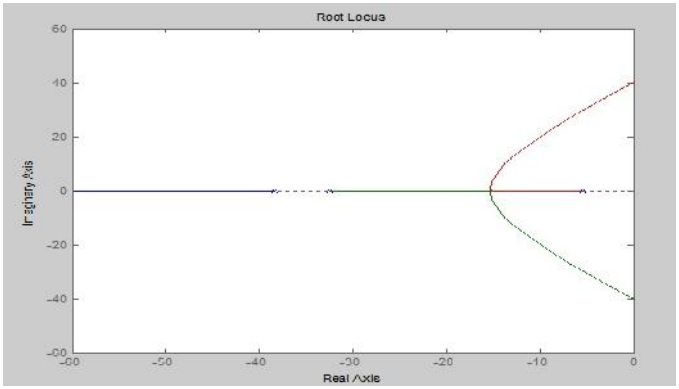

Fig.5: Family of root locus diagram for the conventional droop controller: *DP* = 0.00145, 0.001 ≤ *DQ* ≤0.00433.

However, in this case, it can be observed that the performance of the system is more sensitive to the variation of *DQ* within the same range. In order to obtain satisfied system damping and stability performance, the desired droop gain *DQ* is selected as 0.0143.

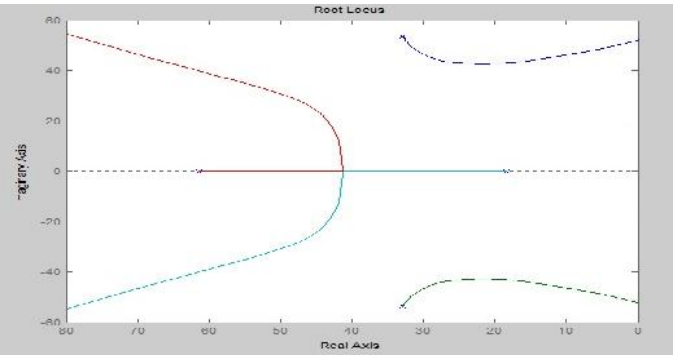

Fig.6: Family of a root locus diagram with the proposed compensation controller: DP = 0.00145, KC = 0.0286, and $0.001 \leq DQ \leq 0.00433$.

Similarly, the response of the system to the integration gain (K_C) variations is examined in Fig. 7. It can also be observed that the stability and damping of the system is sensitive to change of the integration gain. To maintain proper stability and damping features, the selected gain K_C is 0.0286.

From the detailed small-signal analysis, it can be concluded that the stability and damping performance of the microgrid is affected during the compensation process. This phenomenon is very similar to the situation of reactive power tracking error elimination in the grid-connected mode, where the replacement of conventional reactive power droop controller with the PI controller makes the system performance more sensitive to the control parameter variations [8]. However, as will be demonstrated in the next section, the well-designed control parameter can maintain satisfied stability and damping performance during both steady-state operation and compensation transients.

IV RESULTS AND DISCUSSION

A networked microgrid model has been established using MATLAB/Simulink. As shown in Fig. 7, the simulated microgridis composed of three identical DG units and two linear loads. With the same power rating, three DG units shall share the load equally. The detailed configuration of the DG unit is presented in Fig. 8, where an *LC* filter is placed between the IGBT bridge outputs and the DG feeders. The DG line current and filter capacitor voltage are measured to calculate the real and reactive powers. In addition, the well-known multiloop voltage controller is employed to track the reference voltage [7], [8] [14]. The circuit and control parameters of the DG unit are listed in Table I.

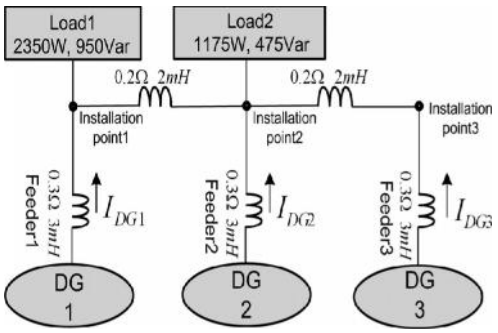

Fig 7: Networked microgrid in the simulation.

TABLE I
DG SYSTEM PARAMETERS

Simulation system	Parameter	Values
Interfaced inverter	Filter resistor, R_f	0.2Ω
Interfaced inverter	Filter inductor, L_f	5mH
Microgrid parameter	Filter capacitor, C_f	40μF
Microgrid parameter	Rated RMS voltage (lint to line)	208V
Droop coefficients	Total load	3525W-1425Var
Droop coefficients	Frequency droop, D_P	0.00125 Rad/ sec.W
Droop coefficients	Voltage droop, D_Q	0.00143V/ Var

Droop coefficients	Integration dead band	6W
Droop coefficients	Integral gain, K_C	0.0286 V/sec.W
Droop coefficients	LPF timeconstant, τ	0.0159 sec
Microgrid parameter	Frequency	60Hz

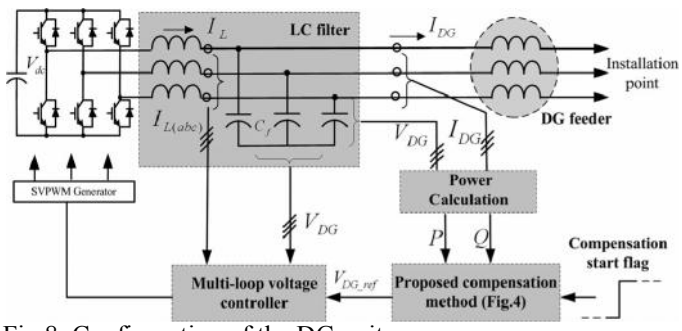

Fig.8: Configuration of the DG unit.

Fig. 9 demonstrates the reactive power flow of the DG units. Due to the unequal voltage drops on networked microgrid feeders, there are significant reactive power errors with the conventional droop control method. On the other hand, the proposed compensation method starting at 1.0 s can effectively adjust the reactive power sharing error to almost zero.

Fig. 10 shows the real power flow of these DG units. Before the compensation, the real power is evenly shared with the conventional droop method. When the compensation is enabled at 1.0 s, due to the transient real and reactive power coupling introduced by (8) and (9), there are some disturbances in the real power. However, the output real power goes back to the original value at around 2.3 s.

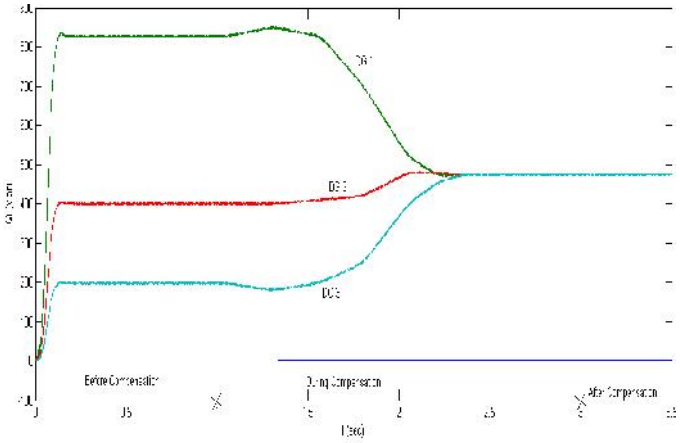

Fig. 9: Simulated reactive power sharing performance in a network microgrid when compensated is activated at 1s

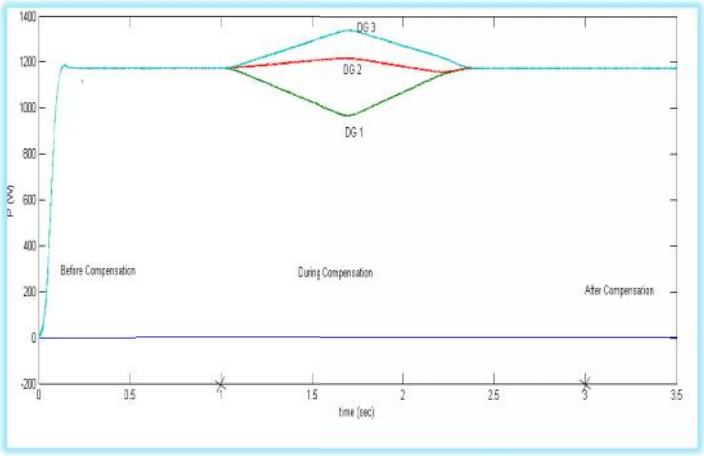

Fig.10: Simulated real power sharing performance in a network microgrid when compensated is activated at 1s

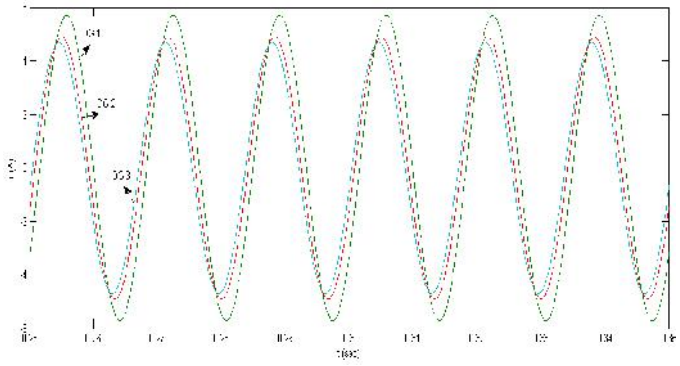

Fig. 11: Simulated DG currents before compensation.

Figs. 11 and 12 show the associated DG line

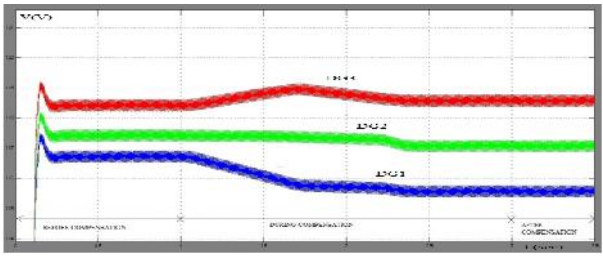

currents. With the conventional droop control method, the magnitude and phase of DG currents are not the same as illustrated in Fig. 11.

Consistent with the power sharing analysis, the DG line currents in Fig. 12 are almost identical after the compensation.

The voltage magnitudes at different locations of the microgrid are also obtained. Fig. 13 shows the changes of DG unit voltage magnitudes during this process. In order to realize equal reactive power sharing, these voltages have small deviations during the compensation. This is because the unequal voltage drops on the feeders are compensated by the DG units.

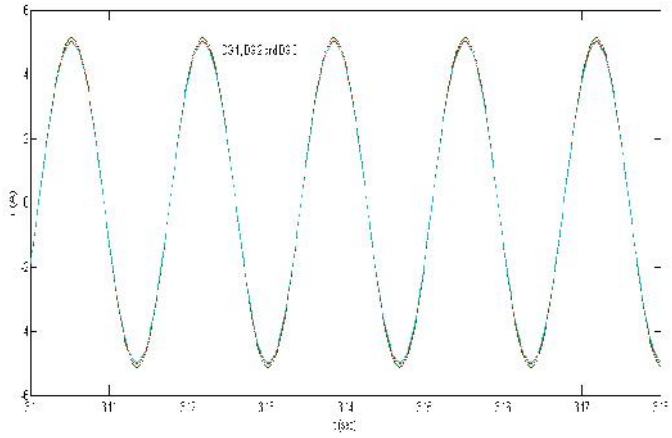

Fig. 12: Simulated DG currents after compensation.

The voltage magnitudes at the installation points (see Fig. 7) are also obtained in Fig. 14. Similar to Fig. 13, these voltage magnitudes also have slight deviations during the compensation.

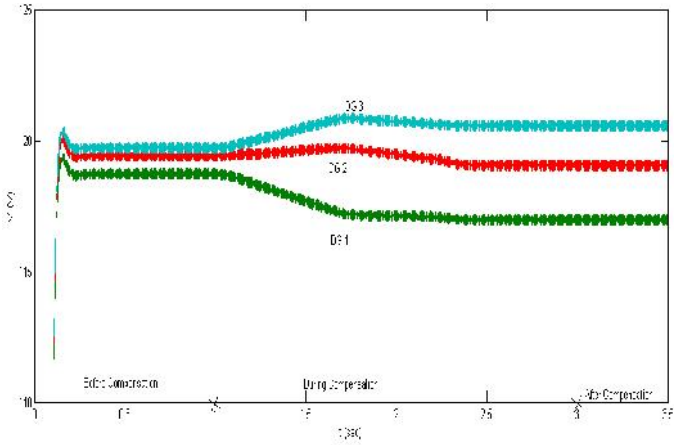

Fig. 13: Simulated DG voltage magnitudes

Fig. 14: Simulated installation points voltage magnitudes.

V CONCLUSION

This project mainly focused on an enhanced control strategy for the accurate reactive power sharing in a multi-DG microgrid, which injects a real-reactive power transient coupling term to identify the errors of reactive power sharing and then compensates the errors using a slow integral term for the DG voltage magnitude control. The compensation strategy also used a low-bandwidth flag signal from the microgrid central controller to activate the compensation of all DG units in a synchronized manner. Therefore, accurate power sharing was achieved without any physical communications among DG units.

In order to investigate the stability of DG units during the compensation process, small-signal analysis method was applied. Root locus diagrams are obtained from the characteristic equations of conventional droop and proposed controlling method which shows that well-designed control parameters frequency droop, voltage droop, and integral gain maintain satisfied stability during steady-state operation and compensation process.

REFERENCES

[1] A. Mehrizi-Sani and R. Iravani, "Potential-function based control of a microgrid in islanded and grid-connected modes," *IEEE Trans. Power Syst.*, vol. 25, no. 4, pp. 1883–1891, Nov. 2010.

[2] K. D. Brabandere, B. Bolsens, J. V. D. Keybus, A.Woyte, J. Drisen, and R. Belmans, "A voltage and frequency droop control method for parallel inverters," *IEEE Trans. Power Electron.*, vol. 22, no. 4, pp. 1107–1115, Jul. 2007.

[3] Y. Li and Y.W. Li, "Power management of inverter interfaced autonomous microgrid based on virtual frequency-voltage frame," *IEEE Trans. Smart Grid.*, vol. 2, no. 1, pp. 30–40, Mar. 2011.

[4] A. Tuladhar, H. Jin, T. Unger, and K.Mauch, "Control of parallel inverters in distributed AC power system with consideration of line impedance effect," *IEEE Trans. Ind. Appl.*, vol. 36, no. 1, pp. 131–138, Jan./Feb. 2000.

[5] C.-T. Lee, C.-C. Chu, and P.-T. Cheng, "A new droop control method for the autonomous operation of distributed energy resource interface converters," in *Proc. Conf. Rec.*

IEEE Energy Convers. Congr. Expo., Atlanta, GA, 2010, pp. 702–709.

[6] J. M. Guerrero, L. G. Vicuna, J. Matas, M. Castilla, and J. Miret, "Output impedance design of parallel-connected UPS inverters with wireless load sharing control," *IEEE Trans. Ind. Electron.*, vol. 52, no. 4, pp. 1126– 1135, Aug. 2005.

[7] J. M. Guerrero, L. G. Vicuna, J. Matas, M. Castilla, and J. Miret, "A wireless controller to enhance dynamic performance of parallel inverters in distributed generation systems," *IEEE Trans. Power Electron.*, vol. 19, no. 4, pp. 1205–1213, Sep. 2004.

[8] Y. W. Li and C.-N. Kao, "An accurate power control strategy for power electronics- interfaced distributed generation units operation in a low voltage multi-bus microgrid," *IEEE Trans. Power Electron.*, vol. 24, no. 12, pp. 2977–2988, Dec. 2009.

[9] J. He and Y. W. Li, "Analysis, design and implementation of virtual impedance for power electronics interfaced distributed generation," *IEEE Trans. Ind. Appl.*, vol. 47, no. 6, pp. 2525–2538, Nov./Dec. 2011.

[10] E. A. A. Coelho, P. C. Cortizo, and P. F. D. Garcia, "Small-signal stability for parallel-connected inverters in stand-alone AC supply systems," *IEEE Trans. Ind. Appl.*, vol. 38, no. 2, pp. 533–542, Mar./Apr. 2002.

[11] N. Pogaku, M. Prodanovic, and T. C. Green, "Modeling, analysis and testing of autonomous operation of an inverter-based microgrid," *IEEE Trans. Power Electron.*, vol. 22, no. 2, pp. 613–625, Mar. 2007.

[12] Y.W. Li, D. M. Vilathgamuwa, and P. C. Loh, "Design, analysis and real time testing of a controller for multibus microgrid system," *IEEE Trans. Power Electron*, vol. 19, no. 5, pp. 1195–1204, Sep. 2004.

[13] J. A. Jardini, C. M. V. Tahan, M. R. Gouvea, S. U. Ahn, and F. M. Figueiredo, "Daily load profiles for residential, commercial and industrial low voltage consumers," *IEEE Trans. Power Del.*, vol. 15, no. 1, pp. 375–380, Jan. 2000.

[14] D. N. Zmood and D. G. Holmes, "Stationary frame current regulation of PWM inverters with zero steady-state error," *IEEE Trans. Power Electron.*, vol. 18, no. 3, pp. 814–822, May 2003.

[15] J. M. Guerrero, J. C. Vasquez, J. Matas, L. G. de Vicuna, and M. Castilla, "Hierarchical control of droop-controlledAC andDCmicrogrids—A general approach toward standardization," *IEEE Trans. Ind. Electron.*, vol. 55, no. 1, pp. 158–172, Jan. 2011.

[16] L. Corradini, P.Mattavelli, M. Corradin, and F. Polo, "Analysis of parallel operation of uninterruptible power supplies though long wiring cables," *IEEE Trans. Power Electron.*, vol. 25, no. 4, pp. 2806–2816, Apr. 2010.

[17] D. De and V. Ramanarayanan, "Decentralized parallel operation of inverters sharing unbalanced and nonlinear loads," *IEEE Trans. Power Electron.*, vol. 25, no. 12, pp. 3015–3025, Dec. 2010.

[18] P.-T. Cheng, C.-A. Chen, T.-L. Lee, and S.-Y. Kuo, "A cooperative imbalance compensation method for distributed generation interface converters," *IEEE Trans. Ind. Appl.*, vol. 45, no. 2, pp. 805–815, Mar./Apr. 2009.

[19] Q. Zhang, "Robust droop controller for accurate proportional load sharing among inverters operated in parallel," *IEEE Trans. Ind. Electron.*, to be published.

[20] J. He and Y. W. Li, "An accurate reactive power sharing control strategy for DG units in a microgrid," in *Proc. 8th Int. Conf. Power Electronics and ECCE Asia*, Jeju, Korea, 2011, pp. 551–556.

[21] V. Gungor, D. Sahin, T. Kocak, S. Ergut, C. Buccella, C. Cecati, and G. Hancke, "Smart grid technologies: Communications technologies and standards," *IEEE Trans. Ind. Inf.*, vol. 7, no. 4, pp. 529–539, Nov. 2011.

[22] E. A. A. Coelho, P. C. Cortizo, and P. F. D. Garcia, "Small signal stability for single phase inverter connected to stiff ac system," in *Proc. Conf. Rec. IEEE-IAS Annu. Meet.*, Oct. 1999, vol. 4, pp. 2180–2187.